

Coexistence of order and chaos at critical points of first-order quantum phase transitions in nuclei

M. Macek and A. Leviatan

Racah Institute of Physics, The Hebrew University, Jerusalem 91904, Israel

We study the interplay between ordered and chaotic dynamics at the critical point of a generic first-order quantum phase transition in the interacting boson model of nuclei. Classical and quantum analyses reveal a distinct behaviour of the coexisting phases. While the dynamics in the deformed phase is robustly regular, the spherical phase shows strongly chaotic behavior in the same energy intervals. The effect of collective rotations on the dynamics is investigated.

Quantum phase transitions (QPTs) are structural changes occurring at zero temperature, resulting from a variation of parameters in the quantum Hamiltonian. They have become a topic of great interest in diverse many-body systems, *e.g.*, atoms, molecules and nuclei. The abrupt changes in the the system's ground state affect the nature of the underlying dynamics and can lead to the emergence of quantum chaos. In the present contribution, we examine this effect in generic (high-barrier) first-order QPTs in nuclei, focusing on the role of the barrier separating the two coexisting phases.¹

We employ the interacting boson model (IBM),² widely used in the description of quadrupole collective states in nuclei, in terms of a system of N monopole (s) and quadrupole (d) bosons, representing valence nucleon pairs. A geometric visualization of the model is obtained by an energy surface, $V(\beta, \gamma)$, which serves as a Landau potential. The latter is defined by the expectation value of the Hamiltonian in the intrinsic condensate state $|\beta, \gamma; N\rangle = (N!)^{-1/2}[\Gamma_c^\dagger(\beta, \gamma)]^N|0\rangle$, where $\Gamma_c^\dagger(\beta, \gamma) = \frac{1}{\sqrt{2}}[\beta \cos \gamma d_0^\dagger + \beta \sin \gamma \frac{1}{\sqrt{2}}(d_2^\dagger + d_{-2}^\dagger) + \sqrt{2 - \beta^2} s^\dagger]$. The quadrupole shape parameters in the intrinsic state characterize the associated equilibrium shape. QPTs have been extensively studied in the IBM.^{3,4} To construct a critical Hamiltonian it is convenient to resolve it into intrinsic and collective parts,⁵

$$\hat{H}_{\text{cri}} = \hat{H}_{\text{int}} + \hat{H}_{\text{col}} . \quad (1)$$

The intrinsic part (\hat{H}_{int}) determines the potential $V(\beta, \gamma)$, while the col-

lective part (\hat{H}_{col}) contains kinetic rotational terms which do not affect its shape. For a first-order critical point, the two parts of the full critical Hamiltonian (\hat{H}_{cri}) can be transcribed in the form⁶

$$\hat{H}_{\text{int}} = \bar{h}_2 P_2^\dagger(\beta_0) \cdot \tilde{P}_2(\beta_0) , \quad (2a)$$

$$\hat{H}_{\text{col}} = \bar{c}_3 \left[\hat{C}_{O(3)} - 6\hat{n}_d \right] + \bar{c}_5 \left[\hat{C}_{O(5)} - 4\hat{n}_d \right] + \bar{c}_6 \left[\hat{C}_{O(6)} - 5\hat{N} \right] . \quad (2b)$$

Here $P_{2\mu}^\dagger(\beta_0) = \beta_0 s^\dagger d_\mu^\dagger + \sqrt{7/2} (d^\dagger d^\dagger)_\mu^{(2)}$, \hat{n}_d (\hat{N}) is the d -boson (total) number operator and \hat{C}_G denotes the quadratic Casimir of the group G as defined in Ref. 5. Barred parameters imply scaling by $N(N-1)$. For $\beta_0 > 0$, \hat{H}_{cri} annihilates both the spherical s -condensate, $|\beta = 0, \gamma; N\rangle$, and the deformed condensate, $|\beta = \beta_e = \sqrt{2}\beta_0(1 + \beta_0^2)^{-1/2}, \gamma = 0; N\rangle$ which correspond to the two coexisting shape phases of the nucleus.

The classical limit of the IBM Hamiltonian is obtained through the use of Glauber coherent states and taking $N \rightarrow \infty$.⁷ The resulting classical image of \hat{H}_{cri} contains complicated expressions, including square roots of polynomials in the coordinates β, γ and their conjugate momenta p_β, p_γ . Setting all momenta to zero, leads to the potential

$$V_{\text{cri}}/h_2 = \frac{1}{2}\beta_0^2\beta^2 + \frac{1}{4}(1 - \beta_0^2)\beta^4 - \frac{1}{2}\beta_0\sqrt{2 - \beta_0^2}\beta^3 \cos 3\gamma . \quad (3)$$

The potential has a spherical minimum at $\beta = 0$ degenerate with a prolate-deformed minimum at $(\beta = \beta_e, \gamma = 0)$ both at energy $V_{\text{min}} = 0$. The barrier, separating the two minima, is located at $\beta = [1 - (1 + \beta_0^2)^{-1/2}]^{1/2}$ and has a height $V_b = h_2[1 - (1 + \beta_0^2)^{1/2}]^2/4$. The limiting value at the domain boundary is $V_{\text{cri}}(\beta = \sqrt{2}, \gamma) = h_2$. The potential can also be expressed in Cartesian coordinates $x = \beta \cos \gamma$ and $y = \beta \sin \gamma$.

Chaotic properties of the IBM have been extensively studied,⁷ albeit, with a simplified Hamiltonian, giving rise to an extremely low, hence non-generic, barrier. To study the effect of the barrier, we consider the classical dynamics associated with \hat{H}_{int} (2a) constrained to $L = 0$. The Poincaré sections for $\beta_0 = 1.0, 1.3, 1.5$, are displayed in Fig. 1. The three cases correspond to “low”, “medium” and “high” potential barriers $V_b/h_2 = 0.04, 0.10, 0.16$, (compared to $V_b/h_2 = 0.0009$ in previous works⁷). The sections are plotted at energies $E_1 = V_b/4$, $E_2 = V_b$ and $E_3 = 4V_b$. In all cases, the motion is predominantly regular at low energies and gradually turning chaotic as the energy increases. However, the classical dynamics evolves differently in the vicinity of the two wells. The family of regular trajectories near the deformed minimum forms a simple pattern of concentric loops around a single stable (elliptic) fixed point. The trajectories remain regular even at

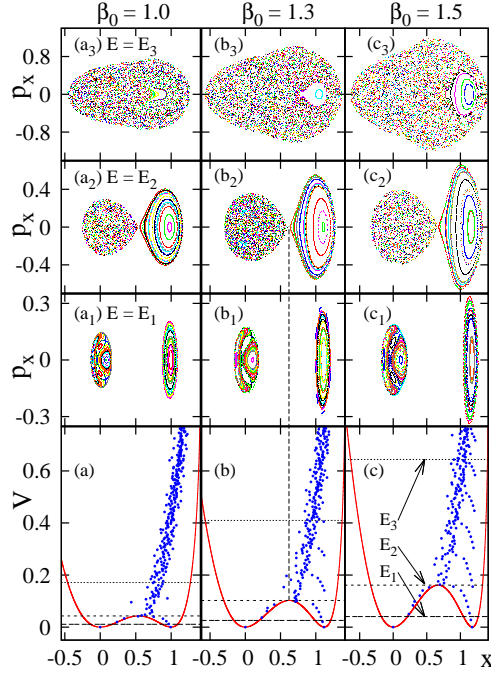


Fig. 1. Poincaré sections at energies E_k (panels a_k - b_k - c_k , $k = 1$ -3) and Peres lattices of ($N = 80$, $L = 0$) eigenstates of \hat{H}_{int} (2a) overlaid on the classical potential $V_{\text{cri}}(x, y = 0)$ for $\beta_0 = 1.0, 1.3, 1.5$ and $h_2 = 1$. Notice the well-separated regular and chaotic dynamics associated with the deformed ($x > 0$) and spherical ($x = 0$) minima, respectively.

energies $E \gg V_b$ (panels a_3 - b_3 - c_3). In contrast, near the spherical minimum, a more complex regular dynamics at low energies (panels a_1 - b_1 - c_1), turns chaotic at a much lower energy ($E \approx V_b/3$) and complete chaoticity is reached near the barrier top. The clear separation between regular and chaotic dynamics, associated with the two minima, persists all the way to $E = V_b$, (panels a_2 - b_2 - c_2). In general, the regularity is more pronounced for higher barriers (larger β_0). These attributes are present also in the quantum analysis in terms of Peres lattices,⁸ formed by the set of points $\{x_i, E_i\}$, with $x_i = \sqrt{2\langle i|\hat{n}_d|i\rangle/N}$, and E_i the energy of the eigenstate $|i\rangle$. The Peres lattices for $L = 0$ eigenstates of \hat{H}_{int} (2a) are shown in the bottom row in panels (a-b-c), nested within the Landau potential $V(x, y = 0)$. For each β_0 , one can clearly identify several regular sequences of states localized in and above the respective deformed wells. A close inspection reveals that their x_i -values lie in the intervals of x -values occupied by the regular tori

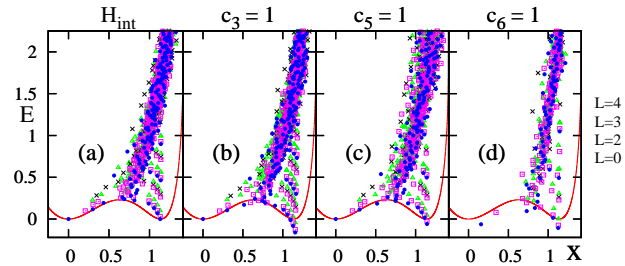


Fig. 2. Peres lattices for eigenstates with $N = 50$, $\beta_0 = 1.35$, $h_2 = 1$ and $L = 0, 2, 3, 4$ of \hat{H}_{int} (2a) (panel a) and additional collective terms (2b) involving $O(3)$, $O(5)$ and $O(6)$ rotations (panels b-c-d), respectively. Notice the well-defined rotational bands ($K = 0$, $L = 0, 2, 4$) and ($K = 2$, $L = 2, 3, 4$) formed by the regular states in the deformed phase shown in panels (a, b, c), which are distorted in panel (d).

in the Poincaré sections. In contrast, the remaining states, including those residing in the spherical minimum, do not show any obvious patterns and lead to disordered (chaotic) meshes of points at high energy $E > V_b$.

Fig. 2 displays combined Peres lattices for eigenstates with $N = 50$, $\beta_0 = 1.35$ and $L = 0, 2, 3, 4$ of \hat{H}_{int} (2a) (panel a) supplemented with three different additional collective terms (2b) $\{c_3, c_5, c_6\} = \{1, 0, 0\}$, $\{0, 1, 0\}$ and $\{0, 0, 1\}$ in panels (b, c, d), respectively. The regular sequences of $L = 0$ eigenstates, mentioned previously in relation to Fig. 1, are seen to be bandhead states of ($K = 0$, $L = 0, 2, 4$) rotational bands of states with nearly equal values of $\langle \hat{n}_d \rangle$. Similarly, sequences of $L = 2, 3, 4$ states form $K = 2$ bands. Such ordered band structures are not present in the chaotic parts of the lattice. The ordered band structure is well preserved by the $O(3)$ and $O(5)$ terms but is suppressed by the $O(6)$ term.

This work is supported by the Israel Science Foundation.

References

1. M. Macek and A. Leviatan, *Phys. Rev. C*, in press (2011).
2. F. Iachello and A. Arima, *The Interacting Boson Model* (Cambridge University Press, Cambridge, 1987).
3. F. Iachello, *Rivista Nuovo Cimento* **34**, 617 (2011).
4. P. Cejnar, J. Jolie and R. F. Casten, *Rev. Mod. Phys.* **82**, 2155 (2010).
5. A. Leviatan, *Ann. Phys. (NY)* **179**, 201 (1987).
6. A. Leviatan, *Phys. Rev. C* **74**, 051301(R) (2006).
7. N. Whelan and Y. Alhassid, *Nucl. Phys. A* **556**, 42 (1993).
8. A. Peres, *Phys. Rev. Lett.* **53**, 1711 (1984).